

RESEARCH

Open Access



Physiological and transcriptomic analysis of *Spartina alterniflora* in response to imazapyr acid stress

Yaning Liu^{1†}, Zhengmao Li^{2,3†}, Lixia Li¹, Xiangyang Jiang^{2,3}, Chen Gao^{2,3} and Jiqiang Zhao^{1*}

Abstract

As a key aspect of managing of invasive alien species in China, the prevention and control of *Spartina alterniflora* have become an important part of the work in coastal provinces, and imazapyr acid has been gradually applied in the control work due to its advantages of high efficiency and low toxicity. In this study, we applied 6.0 L/acre of 25% imazapyr acid aqueous stress treatment, and determined and analyzed the physiological activities and transcriptome profiles of *S. alterniflora* under sustained stress. Chlorophyll fluorescence was used as a technical tool to analyze the mechanism of photosynthesis and the photosynthetic physiological status of *S. alterniflora*. We analyzed the root system structure of *S. alterniflora* using a root system imaging system, and characterized the transcriptome of *S. alterniflora* by high-throughput sequencing technology. Specifically, after imazapyr acid exposure, the fluorescence imaging area of leaves were all decreased, and the fluorescence indexes such as Fv/Fm, Y(II) and Plabs were significantly decreased, while Y(NO) was significantly increased, and Y(NPQ) showed an increase followed by a decrease. Meanwhile, total root length, root surface area and biomass of *S. alterniflora* were suppressed after imazapyr acid exposure. In transcriptomic analysis, imazapyr acid inhibited the expression of genes involved in phenylpropanoid biosynthesis, nucleotide sugar-related metabolism, valine, leucine and isoleucine biosynthesis, and DNA replication in *S. alterniflora*. These results indicate that the effects of imazapyr acid stress on the leaves of *S. alterniflora* are heterogeneous, with the leaves initiating photoprotective mechanisms to ensure the normal functioning of the photosystem in the early stage of stress, and the PSII reaction centers being damaged in the late stage of stress, ultimately destroying the photosynthetic system. Meanwhile, imazapyr acid stress alters basic physiological processes such as metabolism and growth and development of *S. alterniflora*, thus affecting the growth and development of the plant root system, and ultimately leading to the death of *S. alterniflora*.

Keywords *Spartina alterniflora*, Imazapyr acid, Stress response, Chlorophyll fluorescence, Transcriptome

[†]Yaning Liu and Zhengmao Li contributed equally to this work.

*Correspondence:

Jiqiang Zhao
jqzhao@ytu.edu.cn

¹School of Life Science, Yantai University, Yantai, China

²Shandong Marine Resource and Environment Research Institute, Yantai, Shandong 264006, China

³Provincial Key Laboratory of Restoration for Marine Ecology, Laizhou Bay Marine Ecosystem Field Scientific Observation and Research station, Yantai, Shandong 264006, China



Introduction

Spartina alterniflora is native to the Atlantic coast and is a perennial grassy herb [1]. In 1979, *S. alterniflora* was introduced to China as an ecological engineering plant, which rapidly seized the coastal ecological niche due to its extremely strong reproductive and adaptive abilities, and eventually seriously threatening the structure and function of the coastal wetland ecosystem [2, 3]. At present, *S. alterniflora* is included in the list of key management of invasive alien species, and its management has become an important part of management and protecting China's coastal environment.

Chemical control, as a new application technology, plays an increasingly important role in the process of controlling *S. alterniflora* due to its advantages of convenience, high efficiency and low cost, especially environmental friendly herbicides are beginning to be widely tried and applied [4]. Imazapyr acid is a broad-spectrum herbicide of imidazolinones developed by the American Cyanamid Company in the 1980s [5], which is a new type of highly efficient, low-toxic, long-lasting and non-selective post-emergence herbicide with excellent herbicidal activity, mainly targeting grasses, sedge weeds and broad-leaved weeds [6]. The application of imazapyr acid in areas such as the west coast of the US and the Yellow River Delta in China has achieved the purpose of controlling *S. alterniflora* with low short-term environmental risks [7, 8].

Imazapyr acid is a suction-conducting herbicide that has been shown to be absorbed by plant leaves and roots, rapidly transported through the xylem and phloem to plant meristematic tissues and accumulated [9, 10]. Imazapyr acts by inhibiting the enzyme acetohydroxy acid synthase (AHAS), also referred to as acetolactate synthase (ALS) [11]. AHAS catalyzes of the first two reactions of the synthesis of branched-chain amino acids valine, leucine and isoleucine, further interrupting protein synthesis, blocking DNA synthesis and cell growth, and ultimately leading to the loss of greenness of the new leaves and necrosis of the tissues, thus achieving the dual control effect of sexual and asexual reproduction [12, 13]. However, *ahas* gene transcription exhibited tissue-specific divergence, being inhibited in leaves but induced in roots, which may reflect distinct transcriptional regulatory pathways in these tissues [14]. AHAS inhibition either manifests as a result of enhanced plant herbicide metabolism or is due to mutations in the *ahas* gene [15]. However, the detailed mechanism of the response of *S. alterniflora* to imazapyr acid has not been established.

In this study, *S. alterniflora* seedlings were chronically exposed to the herbicide imazapyr acid and physiological and transcriptomic parameters of *S. alterniflora* were monitored. This study aims to (1) elucidate the long-term control effects of imazapyr acid; (2) identify the sensitive

pathways of *S. alterniflora* in response to imazapyr acid stress and reveal the damage process. These results could provide a theoretical basis and data support for the control of *S. alterniflora* by herbicides in coastal wetlands in China.

Materials and methods

Plant materials and chemicals

S. alterniflora seedlings (1–2 leaf stage) and clones (1–3 leaf stage) were obtained from coastal mudflats in Dongying (38°07' N, 118°54' E) and Yantai (37°27' N, 121°39' E), respectively. 25% imazapyr acid water agent was obtained from Shandong Xianda Agrochemicals Co. Ltd. (Shandong, China), and 100% Javelin was obtained from Momentive Performance Materials Ltd. (Waterford, US).

Plant cultivation

The experiment was conducted from May to August 2023 in the experimental field of the College of Life Sciences, Yantai University. Seedlings of *S. alterniflora* with uniform and healthy growth were selected for transplanting. Seedlings were transplanted into 28-hole nursery hole trays (540 mm×310 mm×150 mm), and clones were transplanted into rectangular plastic incubators with drainage holes (650 mm×400 mm×150 mm). The substrate for cultivation was a mixture of peat soil, vermiculite and perlite in a ratio of 4:2:1 (V: V: V). After the survival of seedlings, healthy *S. alterniflora* seedlings at the stage of 4–5 leaves were selected for stem and leaf application, i.e., spraying 6.0 L/acre of 25% imazapyr acid water agent and 0.2 L/acre of organosilicon additives (diluted 56 times).

Chlorophyll fluorescence measurements

The modulated chlorophyll fluorescence imaging system (Imaging PAM, Heinz Walz, Effeltrich, Germany) was used to measure the chlorophyll fluorescence ($n=4$) of cloned seedling leaves at days 0, 1, 3, 7, 17, 30, 45, and 60 under imazapyr acid stress. After 30 min of plants dark adaptation, fully unfolded leaves in the middle and upper layers of the plant were selected and measured. The minimum fluorescence (F_0) was recorded under measuring light, whereas the maximum fluorescence (F_m) was determined at 0.8 s saturation pulse ($2700 \mu\text{mol}\cdot\text{m}^{-2}\cdot\text{s}^{-1}$). When photosynthesis was stabilized, the maximum fluorescence (F_m') after steady-state fluorescence (F_s) and light adaptation was recorded, and then the minimum fluorescence (F_0') under light adaptation was recorded after photochemical light was turned off. Fluorescence parameters were calculated according to the following formulas [16, 17]:

(1) The maximal PSII quantum yield:

$$F_v/F_m = (F_m - F_0)/F_m.$$

(2) Effective quantum yield PSII:

$$Y(II) = (F_m' - F_s) / F_m'$$

(3) Quantum yield of non-regulatory energy dissipation:

$$Y(NO) = F_s / F_m'$$

(4) Quantum yield of regulatory energy dissipation:

$$Y(NPQ) = (F_s / F_m') - (F_s / F_m)$$

Measurement of chlorophyll fluorescence kinetic parameters

Chlorophyll fluorescence rapid induction curves (OJIP curves) of cloned seedling leaves were determined using a multifunctional plant efficiency meter (M-PEA 2, Hansatech, Norfolk, UK) on days 0, 3, 7, 14, 22, 30, 40, 50, 60 and 70 of imazapyr acid stress. The first uppermost fully expanded leaves ($n=8$) were selected and the leaves were dark-adapted for 30 min using acclimatization clips. Induction was performed with $5000 \mu\text{mol}\cdot\text{m}^{-2}\cdot\text{s}^{-1}$ red light, and the fluorescence transients from 10 μs to 1 s were recorded, and fluorescence intensities of F_0 , 150 μs (L-step), 300 μs (K-step), and F_m were measured, and the normalized OJIP parameter differences were calculated separately according to the following equations [18]:

(5) Normalized OJIP parameter differences:

$$\Delta V_{O-P} = \Delta[(F_t - F_0) / (F_m - F_0)]$$

$$\Delta V_{O-K} = \Delta[(F_t - F_0) / (F_L - F_0)]_{\text{Treat}} - [(F_t - F_0) / (F_L - F_0)]_{\text{Control}}$$

$$\Delta V_{O-J} = \Delta[(F_t - F_0) / (F_K - F_0)]_{\text{Treat}} - [(F_t - F_0) / (F_K - F_0)]_{\text{Control}}$$

Other specific parameters can be calculated based on the JIP-test, such as the performance index (PIabs), quantum yield or energy flux ratio (F_v/F_0 , ϕP_0 , ϕE_0 , ϕD_0 , ϕR_0 , δR_0) and specific flux of energy per unit of PSII active reaction center (ABS/RC, REo/RC, TRo/RC, ETo/RC, DIo/RC) [19, 20].

Determination of root system architecture and biomass

On days 0, 7, 14, 21, 28, 42, and 60 of imazapyr acid stress, seedling roots ($n=5$) were slowly removed from the soil with forceps and the roots were thoroughly washed with running water. A plant image analyzer (MICROTEK ScanMaker i800 plus) was used to scan the root system, and root planar geometrical configuration parameters such as total root length, average diameter, root volume, surface area, number of root tips and number of root forks were analyzed by the Wanshen LA-S Series Plant Image Analyzer System.

Plant biomass was determined by the drying method, in which the samples were killed at 105°C for 20 min and dried at 80°C to constant weight to determine the above-ground biomass and below-ground biomass of *S. alterniflora* [21].

Determination of root activity

On days 0, 7, 14, 21, 30, 40, 50, and 60 of imazapyr acid stress, root tips of cloned seedlings ($n=8$) were taken and assayed by the triphenyltetrazolium chloride (TTC) method [22].

Transcriptome profiling of root

Cloned seedling root tissues were collected on days 0, 7, and 30 of imazapyr acid stress (Control, D7, D30) and were immediately frozen in liquid nitrogen with four biological replicates for each treatment. Sequencing was performed by Majorbio Ltd. (Shanghai, China) on the Novaseq 6000 sequencing platform (Illumina, San Diego, US) and raw sequence data were filtered to obtain high-quality data (clean reads). DESeq2 was used for the analysis [23], and genes with $\text{FDR} \leq 0.05$ and $\text{fold-change} \geq 4$ were designated as DEGs. GO and KEGG enrichment analyses were performed using Goatools software [24, 25]. Eight differentially expressed genes were randomly selected for qRT-PCR analysis to validate the high-throughput data ($n=3$). Total RNA was extracted from samples using the SPARKeasy Tissue/Cell RNA Rapid Extraction Kit (AC0201), cDNA was synthesized using the HiScript[®] II Q RT SuperMix for qPCR (+gDNA wiper) (Vazyme) kit, qRT-PCR was performed using the ChamQ Universal SYBR qPCR Master Mix (Vazyme) kit, and primers were synthesized by General Bio (Anhui, China) (Table S1). *SaACTIN* was used as an internal reference gene for all genes, and the expression level of each gene was calculated using the $2^{-\Delta\Delta\text{CT}}$ method [26].

Statistical analysis

All data are presented as means \pm standard deviation (SD) from biological replicates. Data were analyzed by one-way ANOVA and significant difference test ($P < 0.05$) using SPSS 26.0 software (IBM, Chicago, IL, US) and plotted using Origin 2018 (OriginLab, MS, US).

Results

Effects of imazapyr acid stress on chlorophyll fluorescence imaging and parameters

Imazapyr acid stress led to a decrease in the fluorescence imaging area of F_v/F_m , $Y(II)$, $Y(NO)$ and $Y(NPQ)$ of PSII of *S. alterniflora* (Fig. 1A), which was characterized by a decrease in the fluorescence imaging area of the leaves with older leaf age. After imazapyr acid spraying, the photosynthetic activity of *S. alterniflora* leaves changed slowly in the first two weeks. However, the area of photosynthetically active region of the plant decreased rapidly with the prolongation of imazapyr acid stress. The colors representing the magnitude of values in different parts of the same leaf in each fluorescence imaging image of PSII of *S. alterniflora* were not uniform, suggesting that

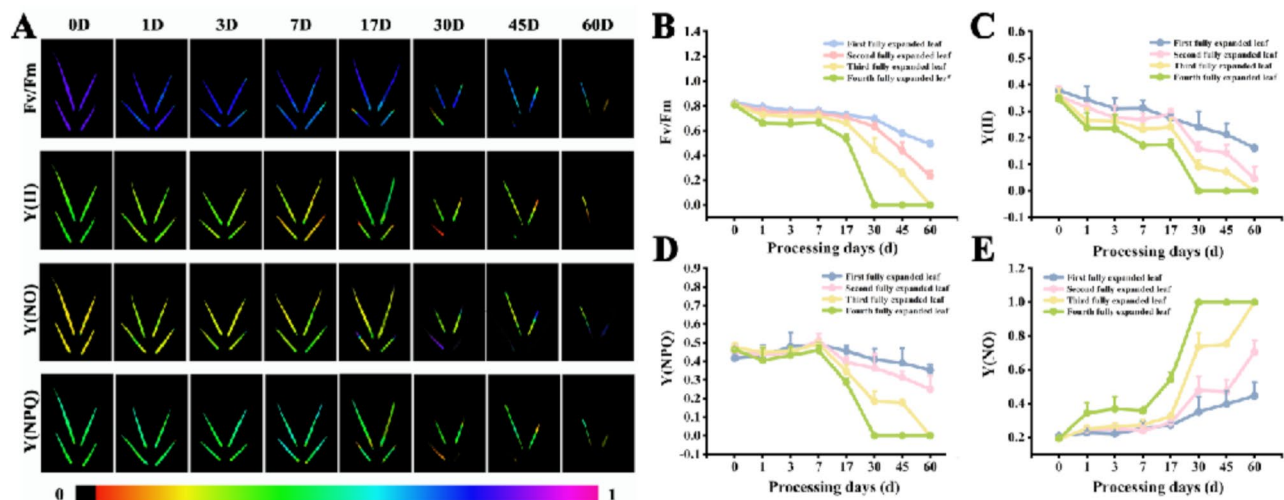


Fig. 1 Changes in chlorophyll fluorescence imaging and parameters under imazapyr acid stress. **(A)** Chlorophyll fluorescence parameter images. The leaves in the figure are the first fully expanded leaf (upper left position), the second fully expanded leaf (upper right position), the third fully expanded leaf (lower left position), and the fourth fully expanded leaf (lower right position). Imazapyr acid stress day 0 is used as control, data reported in the figure are means \pm SD ($n=4$). Each image in the same column represents the same leaf. The color scale at the top indicates values from 0 (black) to 1 (pink). **(B-E)** Changes of **(B)** Fv/Fm. **(C)** Y(II). **(D)** Y(NPQ). **(E)** Y(NO) under imazapyr acid stress

imazapyr acid has a heterogeneous effect on *S. alterniflora* leaves.

Fv/Fm, Y(II), Y(NPQ) and Y(NO) are important parameters for studying plant stress. In this study, imazapyr acid had little effect on the fluorescence indexes of *S. alterniflora* leaves within 7 days of the stress treatment, whereas imazapyr acid significantly decreased Fv/Fm, Y(II), and Y(NPQ) of *S. alterniflora* leaves with the increase of the stress time (Fig. 1B, C and D), and also led to a significant increase in Y(NO) (Fig. 1E). This indicated that imazapyr acid causes damage to the PSII reaction centers of leaves, which in turn disrupts the photosynthetic system. It is also noteworthy that the stress efficiency of imazapyr acid on leaves of different leaf ages was highly variable, with the older the leaf age (fully expanded leaves), the higher the stress efficiency.

Effect of imazapyr acid stress on the kinetic curve of chlorophyll fluorescence

Transient changes in the fast chlorophyll fluorescence signal can reflect the photochemical reaction process in PSII before dark reaction activation. Imazapyr acid stress resulted in a significant increase in the differences between the points of the original OJIP curves (Fig. 2A). The relative fluorescence intensity (F_o) of the O site increased significantly, while the relative fluorescence intensity (F_m) of the P site showed a clear downward trend. The curve flattened out after 30 days, and the line changed significantly after 60 days i.e., to the absence of a distinct O, J, I, and P phases.

To visibly observe the changes in the OJIP curves induced by stress and to identify the effects on the

electron transport chain on the acceptor and donor sides of PSII, the OJIP curves were normalized and the difference in relative fluorescence intensity at each point was calculated. The relative fluorescence intensity V_j of the J phase at 2 ms in the ΔV_{O-P} curve (Fig. 2D), the relative fluorescence intensity V_L of the L phase at 0.15 ms in the ΔV_{O-K} curve (Fig. 2E), and the relative fluorescence intensity V_K of the K phase at 0.3 ms in the ΔV_{O-J} curve (Fig. 2F) increased gradually with the continuation of the stress time, indicating that the PSII donor-side and acceptor-side performance was restricted and destabilized the leaf vesicle-like membrane. At the same time, the increases of V_K and V_j were similar in magnitude, indicating that the donor and acceptor sides of *S. alterniflora* were almost simultaneously injured after spraying imazapyr acid.

With the continuation of imazapyr acid stress time ϕP_o of *S. alterniflora* seedling leaves decreased significantly, and ϕP_o was as low as about 0.1 at 70 days of stress. Meanwhile, PI_{abs} , Fv/Fo, ϕE_o , and ϕR_o of *S. alterniflora* leaves were significantly decreased, and the trend was similar to that of ϕP_o , while ϕD_o and δR_o showed an upward trend. With the increase of imazapyr acid stress time, TR_o/RC , ABS/RC and DIO/RC of *S. alterniflora* seedling leaves showed an increasing trend, while ET_o/RC and Re_o/RC showed a decreasing trend. It indicated that the performance indices, specific activity parameters, and quantum yield and efficiency parameters of the photosynthetic system of the leaves of *S. alterniflora* seedlings were significantly affected by imazapyr acid stress.

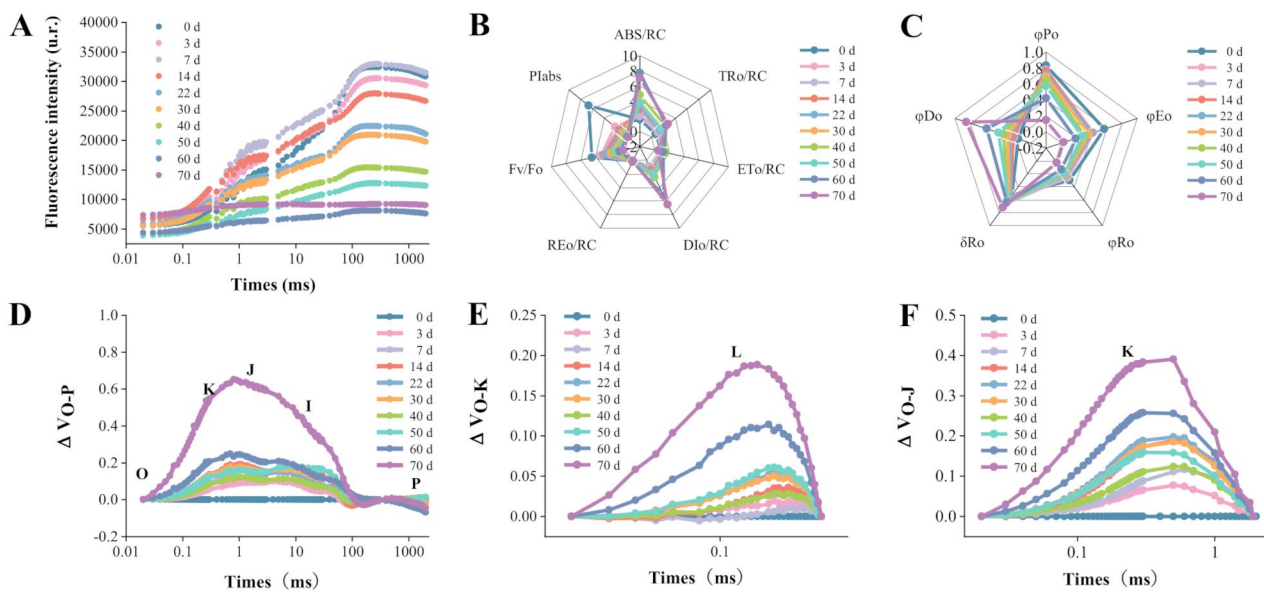


Fig. 2 Changes in chlorophyll fluorescence kinetic curves under imazapyr acid stress. **(A)** The trend of OJIP curves. **(B), (C)** Spider plots of the JIP parameters deduced from chlorophyll a fluorescence OJIP transient curves. **(D)** Trends of O-P standardized difference fluorescence curves. **(E)** Trends of O-K standardized difference fluorescence curves. **(F)** Trends of O-J standardized difference fluorescence curves. Imazapyr acid stress day 0 as control

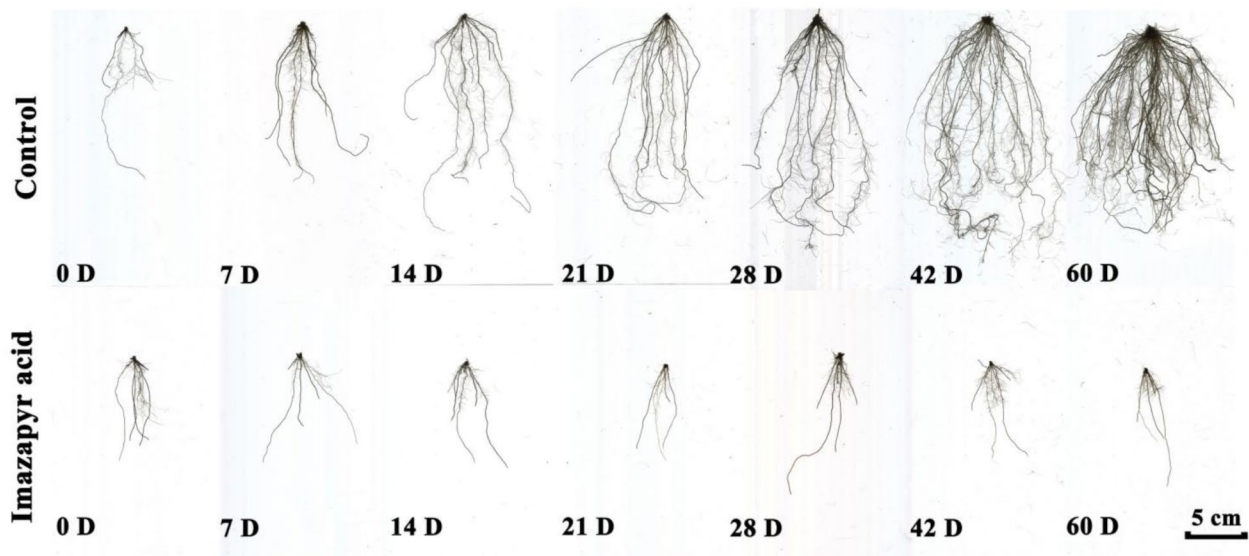


Fig. 3 The scanning images of *S. alterniflora* roots under imazapyr acid stress

Effect of imazapyr acid stress on root system architecture

With the increase of cultivation time, the morphological structure of the root system in the imazapyr acid-treated group and the control group had obvious differences (Fig. 3). The root system of *S. alterniflora* in the control group had a better developed and more branches and relatively complex grading, while after imazapyr acid stress, the root system was relatively simple in grading and the number of roots at all levels was relatively few.

The results indicated that the root growth and development of *S. alterniflora* was significantly inhibited after imazapyr acid stress. Compared to the control, *S. alterniflora* exposed to imazapyr acid stress for 14 days exhibited significant reductions in total root length, root surface area, root volume, number of root tips, and number of root forks, while displaying a marked increase in mean root average diameter (Fig. 4). Furthermore, the differences in these parameters became more significant

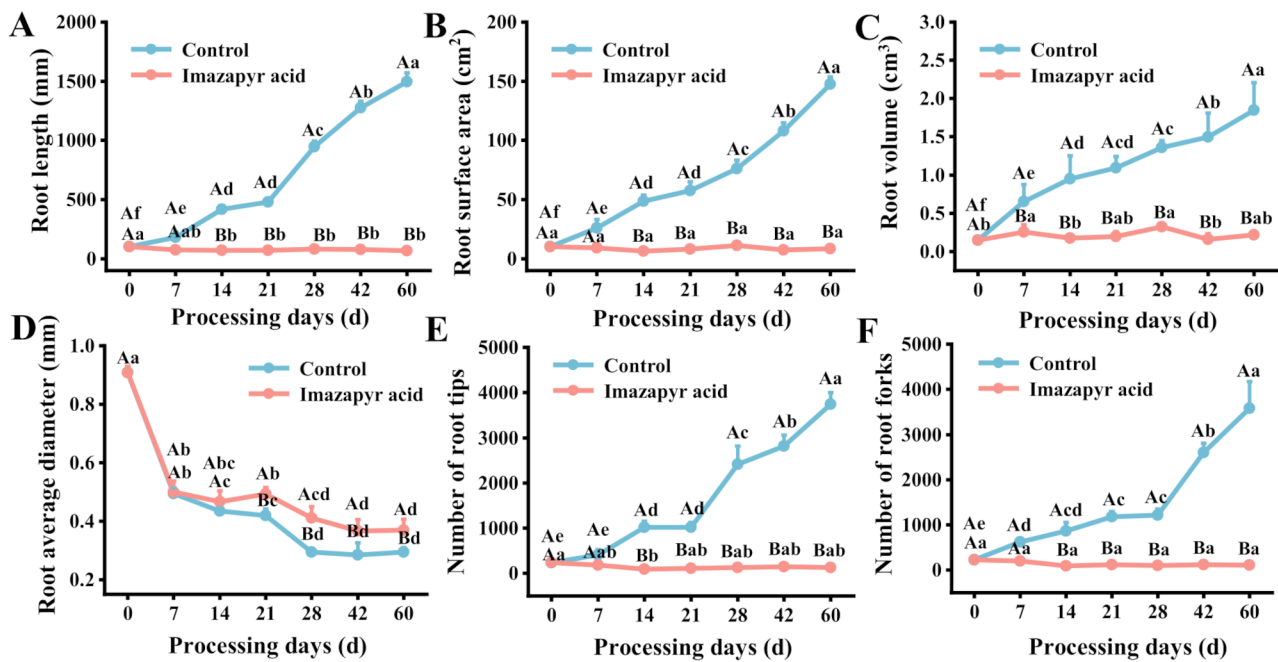


Fig. 4 Root phenotype analysis upon imazapyr acid stress. (A) Root length. (B) Root surface area. (C) Root volume. (D) Root average diameter. (E) Number of root tips. (F) Number of root forks. The water spray treatment was used as the control group. Different lowercase letters mean the significant difference across the time, and uppercase letters mean the significant difference between control and imazapyr acid treatments at the same time

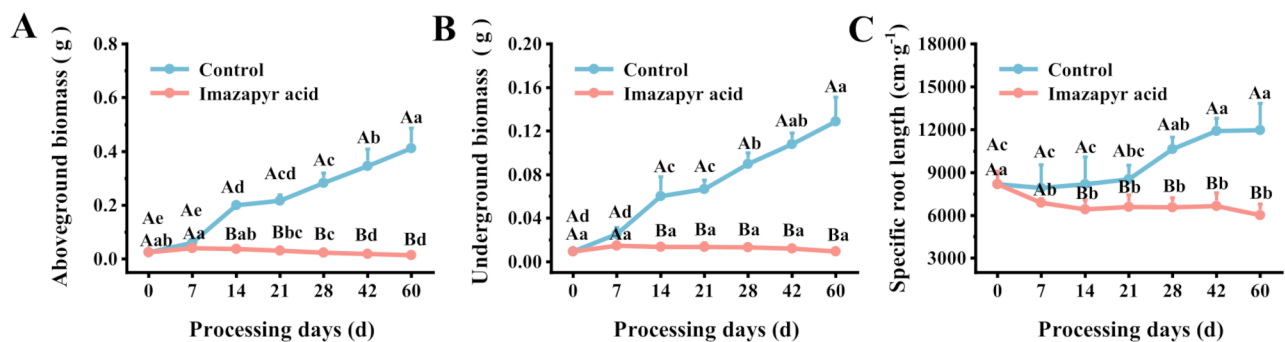


Fig. 5 Effect of imazapyr acid on the biomass and its partitioning of *S. alterniflora*. (A) Aboveground biomass. (B) Underground biomass. (C) Specific root length. The water spray treatment was used as the control group. Different lowercase letters mean the significant difference across the time, and uppercase letters mean the significant difference between control and imazapyr acid treatments at the same time

with prolonged imazapyr acid stress duration. Therefore, imazapyr acid stress can adversely affect the root system and narrow the absorption range of the root system of *S. alterniflora*, thus reducing the efficiency of the root system in absorbing water and nutrients, and further affecting the growth and development of the root system of *S. alterniflora*.

Effect of imazapyr acid stress on root biomass

The accumulation of plant biomass can reflect the plant growth and development, while the specific root length can reflect the ability of the plant root system to absorb water and nutrients. Exposure to imazapyr acid for 14 days markedly suppressed biomass accumulation (both

aboveground and underground) and specific root length in *S. alterniflora* relative to the control, these suppressive effects exhibited a time-dependent escalation under prolonged stress (Fig. 5), which indicated that imazapyr acid stress could significantly inhibit the growth of *S. alterniflora* and affect the ability of the plant to absorb nutrients.

Effect of imazapyr acid stress on root activity

Compared with the control, imazapyr acid stress significantly reduced root vitality as soon as 3 days, completely inactivated the root system around 60 days, and eventually led to the death of the plant root system (Fig. 6). This shows that imazapyr acid can inhibit the growth and

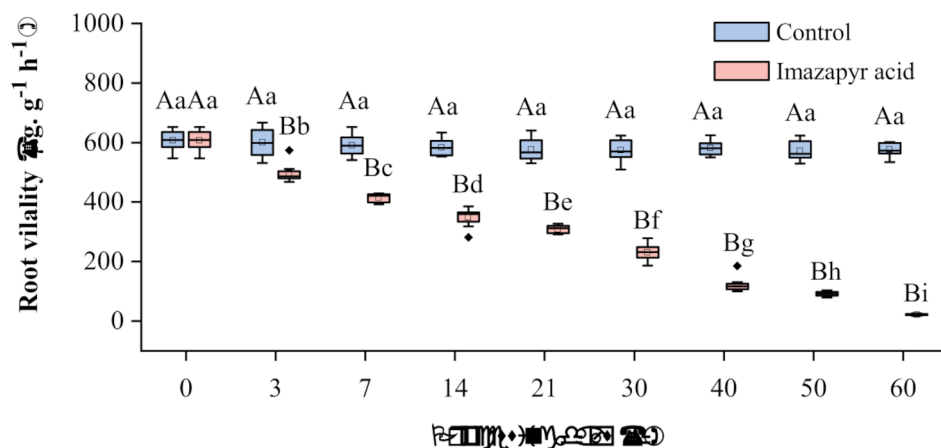


Fig. 6 Changes in root activity under imazapyr acid stress. The water spray treatment was used as the control group. Different lowercase letters mean the significant difference across the time, and uppercase letters mean the significant difference between control and imazapyr acid treatments at the same time

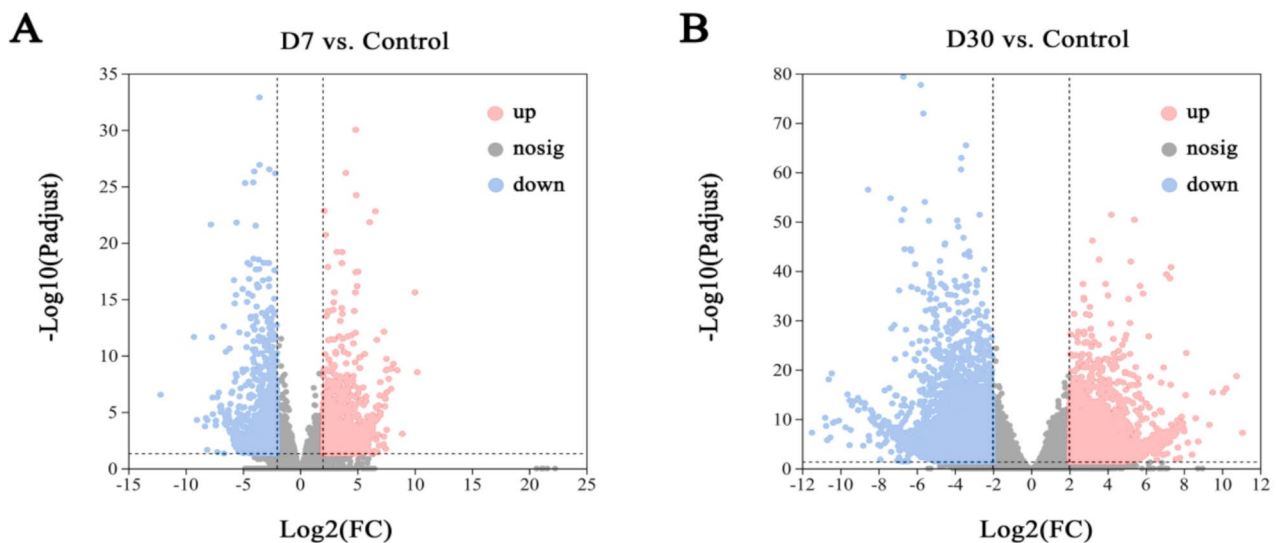


Fig. 7 Volcano plot of differential gene expression analysis. **(A)** D7 vs. Control. **(B)** D30 vs. Control

development of *S. alterniflora* root system by immediately inhibiting plant root activity.

Root transcriptome analysis under imazapyr acid stress

The original sequences obtained from sequencing were all above 4.5 million, and clean reads were obtained after removing low-quality reads, with Q20 and Q30 base percentages above 98% and 94%, respectively, and GC contents greater than 50%, with an error rate of less than 0.025% (Table S2), which indicated that the measured data were of high accuracy and quality, facilitating the subsequent analysis. Differentially expressed gene analysis yielded, a total of 3617 DEGs in D7 vs. Control (Fig. 7A), in which the number of up-regulated genes (2079, 57.5%) was more than the number of down-regulated genes (1538, 42.5%). A total of 11,191 DEGs were

identified in D30 vs. Control (Fig. 7B), of which the number of up-regulated genes was 4858 (43.4%) and the number of down-regulated genes was 6333 (56.6%). On day 7 of imazapyr acid stress, the overall gene regulation of *S. alterniflora* showed a trend of up-regulation. And on day 30 of the stress, the overall gene regulation of *S. alterniflora* showed a trend of down-regulation, which proved that the gene expression regulation of *S. alterniflora* was suppressed in imazapyr acid stress.

The obtained DEGs were GO functionally annotated. The DEGs in D7 vs. Control and D30 vs. Control were annotated into 17 and 20 significant GO terms, respectively (Fig. 8). Under biological processes, cellular process, metabolic process and biological regulation were overrepresented in D7 vs. Control and D30 vs. Control. Under cellular components, the DEGs were mainly

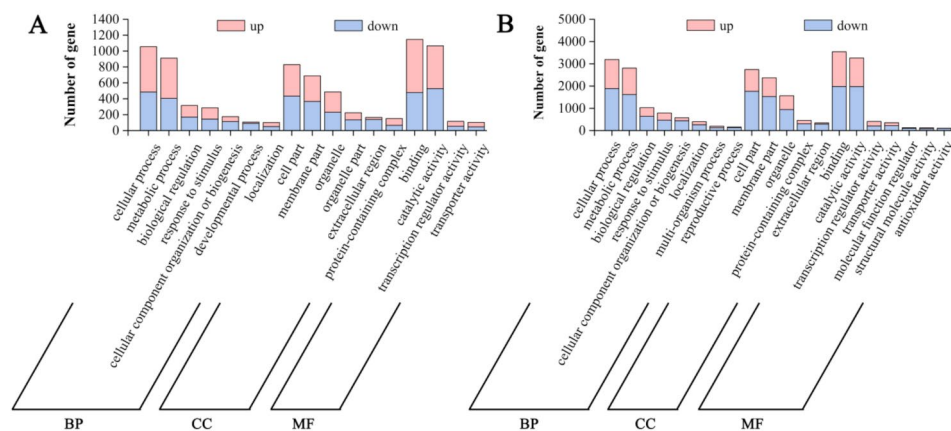


Fig. 8 GO enrichment of DEGs. **(A)** GO classification of DEGs in D7 vs. Control. **(B)** GO classification of DEGs in D30 vs. Control. BP: biological process; MF: molecular function; CC: cellular component. The x-axis represents the most abundant categories of each group, and the y-axis represents the number of the total genes in each category

Table 1 KEGG pathways were significantly enriched in each group

Pathway ID	Pathways	Up	Down	P-value
D7 vs. Control				
map00940	Phenylpropanoid biosynthesis	4	56	2.06E-30
map00073	Cutin, suberine and wax biosynthesis	0	11	1.04E-05
map00520	Amino sugar and nucleotide sugar metabolism	10	18	0.00058786
map04141	Protein processing in endoplasmic reticulum	33	7	0.00087489
map00040	Pentose and glucuronate interconversions	5	7	0.00118822
D7 vs. Control				
map00940	Phenylpropanoid biosynthesis	16	109	6.01E-49
map00073	Cutin, suberine and wax biosynthesis	1	27	2.75E-14
map00460	Cyanoamino acid metabolism	5	32	1.44E-08
map03030	DNA replication	0	35	1.29E-07
map00062	Fatty acid elongation	2	21	8.57E-07
map00999	Biosynthesis of various plant secondary metabolites	9	23	1.28E-06
map00500	Starch and sucrose metabolism	28	47	4.86E-06
map00941	Flavonoid biosynthesis	1	16	7.33E-06
map00520	Amino sugar and nucleotide sugar metabolism	20	45	1.19E-05
map02010	ABC transporters	15	29	1.38E-05
map00100	Steroid biosynthesis	2	21	3.61E-05
map00040	Pentose and glucuronate interconversions	9	16	4.44E-05
map00260	Glycine, serine and threonine metabolism	19	15	6.95E-05
map04075	Plant hormone signal transduction	34	52	0.00013626

annotated in cell membranes, organelles and extracellular regions. In terms of molecular function, the DEGs in both groups were mainly associated with binding, catalytic activity and transcription regulator activity. According to these results, *S. alterniflora* may regulate cellular and metabolic processes to enhance stress tolerance after imazapyr acid stress. However, as the duration of imazapyr acid stress increased, *S. alterniflora* was difficult to maintain normal cell division, differentiation, and other processes through its own regulation, and ultimately inhibited the growth and development of the plant's root system.

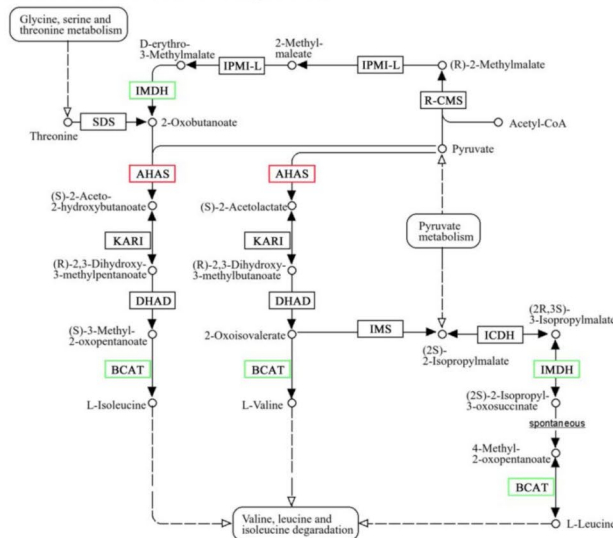
To further understand the metabolic pathways involved in DEGs under imazapyr acid stress in *S. alterniflora*, enrichment analysis was performed using the KEGG database (Table 1). Among them, DEGs in D7 vs. Control and D30 vs. Control were significantly enriched in 5 and 14 metabolic pathways, respectively. There were a total of four metabolic pathways in the two groups, including phenylpropanoid biosynthesis, cutin, suberine and wax biosynthesis amino sugar and nucleotide sugar metabolism and pentose and glucuronate interconversions. Meanwhile, 1 unique pathway was identified as protein processing in the endoplasmic reticulum among

the pathways enriched for DEGs in D7 vs. Control. There were 10 unique pathways in D30 vs. Control, including DNA replication, biosynthesis of various plant secondary metabolites and glycine, serine and threonine metabolism, etc.

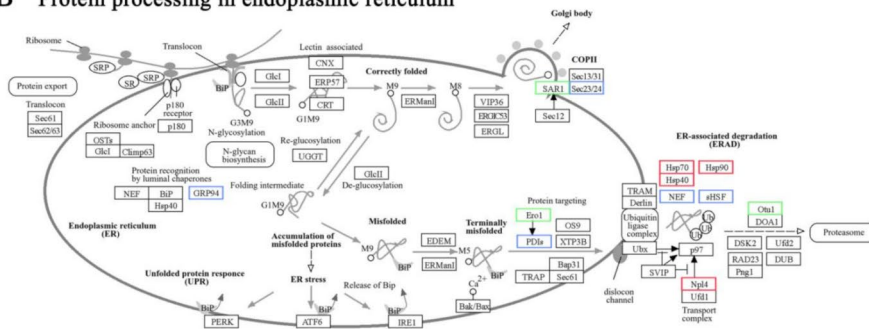
In D7 vs. Control and D30 vs. Control, down-regulation of mainly *leuB* and *ilvE* genes resulted in plants lacking branched-chain amino acid aminotransferases, required

for the pathway, which ultimately affects the process of valine, leucine and isoleucine biosynthesis in *S. alterniflora* (Fig. 9A). During protein processing in the endoplasmic reticulum, the genes encoding *GRp94*, *Sec23* and *Sec24* were oppositely regulated in the two groups, with *HSP90B*, *Sec23*, and *Sec24* showing up-regulation in D7 vs. Control, which helps to segregate misfolded proteins and also helps to mediate protein transport, but the

A Valine, leucine and isoleucine biosynthesis



B Protein processing in endoplasmic reticulum



C DNA replication

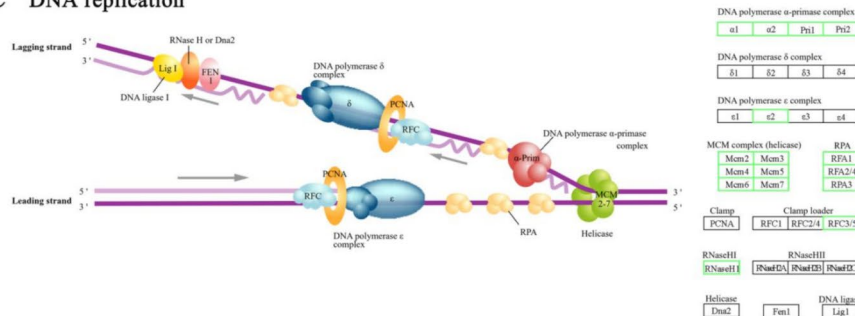


Fig. 9 Map of specific pathways under imazapyr acid stress. **(A)** Valine, leucine and isoleucine biosynthesis. **(B)** protein processing in endoplasmic reticulum. **(C)** DNA replication. Boxes represent enzymes, small circles represent metabolites, and rounded boxes represent another metabolic pathway diagram. Green represents down-regulated gene, red represents up-regulated gene, and blue represents both up- and down-regulated gene. The expression of gene in this figure refers to comprehensive performance among in D7 vs. Control and D30 vs. Control

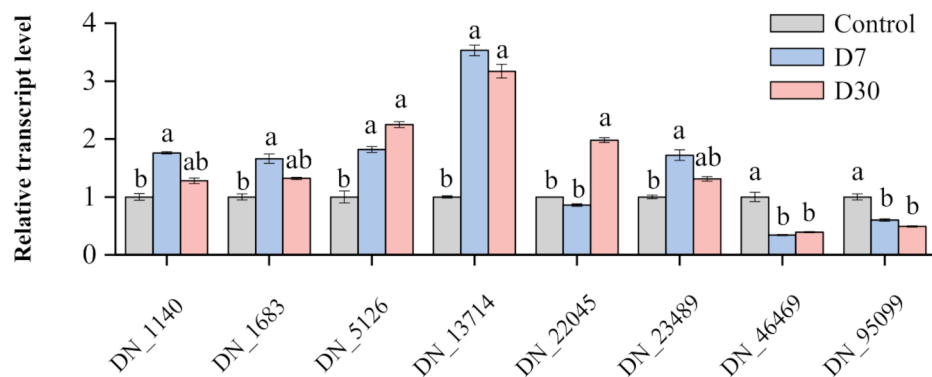


Fig. 10 qRT-PCR verification of target gene expression levels. The different small letters on histogram represent significant difference at $P < 0.05$ among different treatment time

opposite in D30 vs. Control (Fig. 9B). Genes encoding DNA polymerase α -primase complex (pol α -prim), MCM complex and RPA were significantly down-regulated in D30 vs. Control, affecting the process of plant DNA replication (Fig. 9C). In genetic information processing, stress led to the down-regulation of *POLA1*, *POLA2*, *PRI1* and *PRI2* genes, which affected the expression of pol α and primase, resulting in the reduction of pol α -prim synthesis activity. Simultaneous down-regulation of the genes encoding MCM complex, *RPA1*, *RPA2* and *RPA3* affected DNA deconjugase activity as well as the single-stranded DNA binding process.

Experimental validation of DEGs by qRT-PCR

To ensure the reproducibility of the gene expression data, eight genes were randomly selected from the transcriptome sequencing results and validated by qRT-PCR using *SaACTIN* as the internal reference gene. The expression trends of the eight genes measured by qRT-PCR were basically consistent with those of the transcriptome results (Fig. 10, Table S3), which demonstrated the reliability and accuracy of the RNA-seq sequencing results.

Discussion

Since *S. alterniflora* is an invasive plant in coastal wetlands in China, the herbicide selected for control should achieve the purpose of control while ensuring that it is safe for the environment. Therefore, the high efficiency, low toxicity and easily degradable imazapyr acid was used in this study [27]. However, the physiological and molecular responses of this herbicide to *S. alterniflora* is not fully understood. In this study, imazapyr acid stress could severely inhibit the photosynthetic activity of *S. alterniflora* leaves and the growth and development of the root system. Meanwhile, the results of transcriptomics analysis further indicated that imazapyr acid stress affects important physiological processes such as metabolism and DNA replication of *S. alterniflora*.

Impairment of the chlorophyll fluorescence imaging of *S. alterniflora* after imazapyr acid stress

Chlorophyll fluorescence is a very sensitive probe for probing the physiological state of leaves, allowing rapid assessment of plant performance and reflecting the effects of adversity stress on the photosynthetic activity of plant leaves [28]. In particular, chlorophyll fluorescence imaging technology allows two-dimensional imaging of samples while detecting various photosynthetic indicators [29]. Therefore, in the present study, using chlorophyll fluorescence imaging on *S. alterniflora*, there was heterogeneity in the inhibitory effect of imazapyr acid on leaf photosynthetic activity, while the inhibitory effect was more pronounced in the 4th fully expanded leaf, followed by the 3rd, 2nd, and 1st fully expanded leaves, indicating that the greater the leaf age, the greater the degree of photoinhibition. The researchers observed that photosynthetic activity was strongest when the leaves were fully expanded and gradually decreased with leaf senescence [30].

Abiotic stresses generally inhibit plant leaf PSII photochemical efficiency, leading to an increase in the proportion of light energy absorbed by leaves allocated to the unregulated energy dissipation fraction of PSII and the onset of PSII photoinhibition [31, 32]. In this study, we found that in the pre-stress period of imazapyr acid, the leaves of *S. alterniflora* seedlings showed a small decrease in Fv/Fm and Y(II), and a small increase in Y(NPQ) and Y(NO). This indicated that the pre-stress period of imazapyr acid had a relatively small effect on the *S. alterniflora* seedlings, and that the photochemical efficiency of the leaves of the seedlings was reduced but the photoprotective mechanism of the leaves began to be activated, indicating that the photosynthetic system can be induced to maintain higher heat dissipation thereby dissipating the excess light energy absorbed by the leaves for proper functioning of the photosystem. In contrast, at the late stage of imazapyr acid stress, Fv/Fm, Y(II) and Y(NPQ) of

S. alterniflora seedling leaves decreased dramatically, and $Y(NO)$ increased dramatically. This suggests that with the continuation of the stress time, the activity of PSII was reduced, the performance of heat dissipation declined, and ultimately the photosynthetic system was damaged and photoinhibition occurred. F_v/F_m is considered to be a sensitive indicator describing the photosynthetic system's ability to carry out photosynthesis, and it is more stable under non-environmental stress conditions. Usually the value of higher plants is stable at 0.80–0.86, and the PSII active center is completely inactivated when the F_v/F_m fluorescence value of the plant is less than 0.44 [33]. In this study, F_v/F_m of *S. alterniflora* showed a decreasing trend after imazapyr acid stress, indicating that the leaves were photoinhibited, and the older the leaves, the stronger the degree of photoinhibition. The PSII active centers of the 2nd, 3rd, and 4th fully expanded leaves were completely inactivated, but the F_v/F_m of the 1st fully expanded leaf was still greater than 0.44, therefore it is still necessary to further check whether the active center of plant PSII is completely inactivated or not to avoid the condition of regrowth.

Effect of imazapyr acid stress on the kinetic curve of rapid chlorophyll fluorescence induction

The fast chlorophyll fluorescence-induced kinetic curve (OJIP curve) can reflect the changes in processes such as the primary photochemical reaction of PSII and the electron transport state of the photosynthetic apparatus [34]. Dramatic changes in the OJIP curves of *S. alterniflora* leaves after imazapyr acid stress for 30 days implied that imazapyr acid exerted severe effects on PSII reaction centers and the photosynthetic electron transport chain. It was shown that the photosynthetic redox capacity of plants was inhibited and stomatal restriction increased after being stressed by imidazolinone herbicides, which ultimately led to a decrease in the photosynthetic carbon assimilation capacity of plants [35]. Meanwhile, ϕP_o , F_v/F_o and PI_{abs} are important indicators reflecting the light energy conversion efficiency of PSII reaction center and the degree of inhibition of photosynthetic electron transfer [36]. In this study, ϕP_o , F_v/F_o and PI_{abs} were significantly reduced with the continuation of imazapyr acid stress time, indicating that imazapyr acid reduced the number of active PSII reaction centers, lowered the activity of PSII reaction centers, and inhibited the photosynthetic electron transfer rate, which disrupted the energy conservation of electron transfer. Eventually, at 70 days of stress, ϕP_o was reduced to about 0.1, indicating that the photosynthetic activity of all leaves of *S. alterniflora* was completely inactivated and the plant died.

To further investigate the loci of imazapyr acid's effect on the photosynthetic apparatus of *S. alterniflora* leaves and its mechanism [37, 38], the present study analyzed

the changes in PSII reaction centers, donor side and acceptor side. In this study, V_L , V_K , V_J , and V_I of leaves were significantly increased after imazapyr acid stress, indicating that imazapyr acid impaired the oxygen-excreting complex (OEC) on the donor side of PSII, inhibited the electron-transferring ability on the acceptor side as well as the acceptance of electrons by the PQ pools, and destabilized the leaf vesicle-like membranes. Meanwhile, ϕR_o and ϕE_o were both reduced by about 90% at 70 days of imazapyr acid stress treatment compared with the pre-stress period, indicating that imazapyr acid significantly disrupts both PSII receptor-side and PSI electron transport.

In addition, according to the energy flow model, most of the energy absorbed by the antenna pigments was captured by the reaction centers and drove electron transfer, while the rest was dissipated in the form of heat or fluorescence [39]. After imazapyr acid stress, ABS/RC , TR_o/RC , and DI_o/RC of leaves increased, while ET_o/RC decreased, indicating that the light energy absorbed and captured by antennal pigments increased, but the energy used for electron transfer decreased. It has been shown that abiotic stress-induced plant senescence leads to an increase in the amount of energy absorbed per reaction center (ABS/RC), which causes an increase in the excitation pressure of the reaction center (DI_o/RC) [40]. Therefore, imazapyr acid stress may further lead to leaf senescence by inhibiting the photosynthetic performance of *S. alterniflora*, causing degradation of leaf cellular fractions and ultimately leading to cell death.

Inhibition of root growth and development of *S. alterniflora* after imazapyr acid stress

The plant root system is an important nutrient organ, which can absorb, store and transport nutrients needed by plants for normal growth [41]. When plants are subjected to stress, the morphology and physiological characteristics of the root system are affected to varying degrees, which are often characterized by changes in root morphology and reduced biomass [42]. Therefore, in this study, the root growth of *S. alterniflora* seedlings was analyzed after stress, and the total root length, average root diameter, root volume and specific root length of the root system were significantly inhibited after imazapyr acid stress, but none of them changed significantly after one week of stress. It has also been shown that plants under abiotic stress use more assimilates for aboveground growth and reproduction, with less input to the root system [43]. In this study, aboveground biomass increased significantly but underground biomass did not change significantly during the pre-stress period of imazapyr acid, and both aboveground and underground biomass of *S. alterniflora* were significantly suppressed during the later stage of stress. The results showed that

imazapyr acid immediately affected the root growth and development of solid seedlings of *S. alterniflora*, including impeded development of fine roots, reduced nutrient utilization efficiency, and significant inhibition of root proliferation, as well as inhibition of the growth of the upper portion of the *S. alterniflora* ground and ultimately led to the death of *S. alterniflora*.

Transcriptome response to imazapyr acid exposure

It was found that imazapyr acid can be taken up by the root system of plants and rapidly passes through xylem and phloem entry to accumulate in the phloem tissues [44], therefore, the present study was conducted to further investigate the mechanism of root response to imazapyr acid. AHAS is the first enzyme in the branched-chain amino acid (BCAA) biosynthesis pathway and catalyzes the production of L-valine, L-leucine and L-isoleucine [45], but no significant change in AHAS activity was detected in the transcriptome assay. It has been shown that herbicides mainly act at 3–8 h of application, and the expression level of AHAS may be significantly affected during this period of time [46]. However, with the continuation of the stress time, the expression of this gene may no longer be significantly suppressed. In valine, leucine and isoleucine biosynthesis, amino acid synthesis is affected mainly through the down-regulation of *leuB* and *ilvE*. It was found that the deletion of the *ilvE* gene could directly lead to the reduction of the synthesis ability of branching amino acids (Val, Ile, Leu), which affects the growth of plants, while the lack of *LeuB* also causes the activation of protease activity and autophagy through leucine depletion [47]. It is also noteworthy that the elevated expression of AHAS in D30 vs. Control may be due to a negative feedback mechanism of the product modulating the activity of the AHAS enzyme [48]. In addition, amino acids are essential substrates for protein biosynthesis in cells, and inhibition of amino acid synthesis further affects nitrogen metabolic pathways and the regulation of carbon and nitrogen balance in plants [49]. Therefore, imazapyr acid stress may lead to the disruption of nitrogen metabolism pathways in *S. alterniflora*, manifested through nitrogen deficiency symptoms characterized by structural damage to mitochondria in root cells, protein denaturation, and cytoplasmic acidosis. These pathological alterations collectively inhibit root system development and ultimately lead to root system mortality. Meanwhile, the blocked nitrogen metabolism may further affect leaf growth and development, manifesting as chlorosis. Notably, one month post-imazapyr acid exposure, this metabolic impairment may inhibit photosynthetic activity through rapid reduction of chlorophyll fluorescence parameters in leaves. These changes accelerate photoinhibition progression, which ultimately culminates in leaf senescence and mortality.

DEGs under imazapyr acid stress were mainly enriched in phenylpropanoid biosynthesis, cutin, suberine and wax biosynthesis and amino sugar and nucleotide sugar metabolism. The phenylpropanoid biosynthesis pathway is an important metabolic pathway responsible for the synthesis of a wide range of secondary metabolites, which begins with phenylalanine and ultimately produces a variety of phenylpropanoid compounds, such as lignin, flavonoids, and isoflavones [50, 51]. Studies have shown that the phenylpropanoid biosynthesis pathway responds to abiotic stresses in a variety of plants, with lignin deposition playing an important role in plant development and response to abiotic stresses [52, 53]. In this study, DEGs enriched in down-regulated Phenylpropanoid biosynthesis increased with increasing duration of imazapyr acid stress, and the down-regulation of Phenylpropanoid biosynthesis may be related to reduced lignin deposition [54]. Reduced lignin deposition affects the mechanical strength and transport function of the root system, leading to greater sensitivity of the roots to mechanical stimulation of the soil and thus inhibiting plant growth and development [55]. These findings further support the inhibitory effect of imazapyr acid stress on the root growth and development of *S. alterniflora* after one week of stress.

However, it is worth noting that most of the DEGs involved in the DNA replication process were down-regulated in expression, especially the genes encoding Polaprim and MCM2-7 complex, which led to the inhibition of the initiation of DNA synthesis in eukaryotic replication, as well as the instability of the MCM library, which led to abnormal replication fork shift speed and symmetry, inducing endogenous replication stress and DNA damage [56]. If the DNA damage continues to accumulate, it leads to growth inhibition and yield reduction, as well as to the entry of cells into the apoptotic pathway [57], which further explains the inhibition of root growth after imazapyr acid stress.

Conclusions

In this study, imazapyr acid significantly inhibited the photosynthetic activity of *S. alterniflora*, resulting in severe photoinhibition of leaves, and the growth and development of *S. alterniflora*'s root system was significantly inhibited by imazapyr acid. In addition, imazapyr acid inhibited the synthesis of branched-chain amino acids in *S. alterniflora*, affecting the nitrogen metabolism and the regulation of carbon and nitrogen balance in plants; imazapyr acid inhibited the DNA replication process, causing DNA damage, and ultimately leading to the apoptotic pathway of cells. These results indicated that imazapyr acid would seriously interfere with the processes of photosynthesis, metabolism, growth and reproduction of *S. alterniflora*, achieving the dual prevention

and control of sexual and asexual reproduction. The present study revealed the physiological and transcriptomic responses of *S. alterniflora* to imazapyr acid stress, providing data support for the evaluation of imazapyr acid as an effective herbicide to *S. alterniflora*, as well as some theoretical basis for future management of *S. alterniflora*.

Supplementary Information

The online version contains supplementary material available at <https://doi.org/10.1186/s12870-025-06659-8>.

Supplementary Material 1

Author contributions

YL: Writing—original draft, Investigation, Data curation. ZL: Writing—original draft, Investigation, Data curation. LL: Investigation, Data curation. XJ: Writing—review & editing, Funding acquisition, Data curation. CG: review & editing, Funding acquisition, Data curation. JZ: Supervision, Project administration, Conceptualization, Writing—review & editing.

Funding

This study was funded by the Projects “Marine ecological disaster management—Investigation and pilot management of *Spartina alterniflora* in Shandong Province(2020–2023)”.

Data availability

No datasets were generated or analysed during the current study.

Declarations

Ethics approval and consent to participate

No specific permits were needed, and material collection and molecular experiments were performed in accordance with current Chinese regulations.

Consent for publication

Not applicable.

Competing interests

The authors declare no competing interests.

Received: 13 February 2025 / Accepted: 30 April 2025

Published online: 13 May 2025

References

- Lu J, Zhang Y. Spatial distribution of an invasive plant *Spartina alterniflora* and its potential as biofuels in China. *Ecol Eng*. 2013;52:175–81.
- Meng W, Feagin RA, Innocenti RA, Hu B, He M, Li H. Invasion and ecological effects of exotic smooth cordgrass *Spartina alterniflora* in China. *Ecol Eng*. 2020;143:105670.
- Liang Q, Yan Z, Li X. Influence of the herbicide haloxyfop-R-methyl on bacterial diversity in rhizosphere soil of *Spartina alterniflora*. *Ecotoxicol Environ Saf*. 2020;194:110366.
- An SQ, Gu BH, Zhou CF, Wang ZS, Liu YH. *Spartina* invasion in China: implications for invasive species management and future research. *Weed Res*. 2007;47(3):183–91.
- Osuna M, Fischer A, Prado R. Herbicide resistance in *Aster squamatus* conferred by less sensitive form of acetolactate synthase. *Pest Manag Sci*. 2003;59:1210–6.
- Peng H-B, Shi J, Gan X, Zhang J, Ma C, Piersma T, Melville DS. Efficient removal of *Spartina alterniflora* with low negative environmental impacts using Imazapyr. *Front Mar Sci*. 2022; 9:1054402.
- Patten K. Smooth cordgrass (*Spartina alterniflora*) control with Imazapyr. *Weed Technol*. 2009;16:826–32.
- Mo X, Chen J, Pan Y, Zhang M, Zhang Z, Liu J. Impact of applying Imazapyr on the control of *Spartina alterniflora* and its eco-environments in the yellow river delta, China. *Watershed Ecol Environ*. 2022;4:211–8.
- Huripurshad S, Beckett RP, Campbell P. Seasonal variation in acetohydroxy acid synthase Inhibition by Imazapyr in *Cynodon dactylon*. *South Afr J Bot*. 2018;116:82–5.
- Buffon G, Lamb TI, Lopes MCB, Sperotto RA, Timmers LFSM. Push it to the limit: identification of novel amino acid changes on the acetolactate synthase enzyme of rice that putatively confer high level of tolerance to different Imidazolinones. *Front Bioeng Biotechnol*. 2020; 8(73).
- Merriam AA-O, Malone JA-O, Hereward JA-O, Gill G, Preston C. Point mutations including a novel Pro-197-Phe mutation confer cross-resistance to acetolactate synthase (ALS) inhibiting herbicides in *Lactuca serriola* in Australia. *Pest Manag Sci*. 2023;79(12):5333–40.
- Kettenring KM, Adams CR. Lessons learned from invasive plant control experiments: a systematic review and meta-analysis. *J Appl Ecol*. 2011;48:970–9.
- Piao Z, Wang W, Wei Y, Zonta F, Wan C, Bai J, Wu S, Wang X, Fang J. Characterization of an acetohydroxy acid synthase mutant conferring tolerance to imidazolinone herbicides in rice (*Oryza sativa*). *Planta*. 2018; 247(3):693–703.
- Mandal S, Ji W, McKnight TD. Candidate gene networks for acylsugar metabolism and plant defense in wild tomato *Solanum pennellii*. *Plant Cell*. 2020;32(1):81–99.
- Wuddineh WA, Xu X, Zhong G-Y. Amino acid substitutions in grapevine (*Vitis vinifera*) acetolactate synthase conferring herbicide resistance. *Plant Cell Tissue Organ Cult (PCTOC)*. 2023;154(1):75–87.
- Kramer DM, Johnson G, Kierats O, Edwards GE. New fluorescence parameters for the determination of Q_A redox state and excitation energy fluxes. *Photosynth Res*. 2004;79(2):209–18.
- Scholes JD, Rolfe SA. Chlorophyll fluorescence imaging as tool for Understanding the impact of fungal diseases on plant performance: a phenomics perspective. *Funct Plant Biol*. 2009;36(11):880–92.
- Huo J, Song B, Riaz M, Song X, Li J, Liu H, Huang W, Jia Q, Wu W. High Boron stress leads to sugar beet (*Beta vulgaris* L.) toxicity by disrupting photosystem II. *Ecotoxicol Environ Saf*. 2022;248:114295.
- Strasser RJ, Tsimilli-Michael M, Qiang S, Goltsev V. Simultaneous in vivo recording of prompt and delayed fluorescence and 820-nm reflection changes during drying and after rehydration of the resurrection plant *Haberlea rhodopensis*. *Biochim Et Biophys Acta (BBA) - Bioenergetics*. 2010;1797(6):1313–26.
- Mehta P, Allakhverdiev SI, Jajoo A. Characterization of photosystem II heterogeneity in response to high salt stress in wheat leaves (*Triticum aestivum*). *Photosynth Res*. 2010;105(3):249–55.
- Agathokleous E, Belz RG, Kitao M, Koike T, Calabrese EJ. Does the root to shoot ratio show a hormetic response to stress? An ecological and environmental perspective. *J Forestry Res*. 2019;30(5):1569–80.
- Zhang ZY, Bu JJ, Wang SF, Hu GH, Wang QL. Effect of coronatine on cotton root activity determined by TTC assay at different levels of potassium. *Plant Physiol J*. 2015;51(5):695–701.
- Anders S, Huber W. Differential expression analysis for sequence count data. *Genome Biol*. 2010;11(10):R106.
- Young MD, Wakefield MJ, Smyth GK, Oshlack A. Gene ontology analysis for RNA-seq: accounting for selection bias. *Genome Biol*. 2010;11(2):R14.
- Kanehisa M, Araki M, Goto S, Hattori M, Hirakawa M, Itoh M, Katayama T, Kawashima S, Okuda S, Tokimatsu T, et al. KEGG for linking genomes to life and the environment. *Nucleic Acids Res*. 2008;36:D480–484.
- Livak KJ, Schmittgen TD. Analysis of relative gene expression data using real-time quantitative PCR and the 2(-Delta Delta C(T)) method. *Methods*. 2001;25(1046–2023):402–8.
- Levy N, Knott C, Webster E, Hensley J, Blouin D, Yang Y. Chemical control of weeds and genetic Off-Types in smooth cordgrass (*Spartina alterniflora*) production ponds. *Ecol Restor*. 2013;31:19–22.
- Zhang YJ, Gao H, Li YH, Wang L, Kong DS, Guo YY, Yan F, Wang YW, Lu K, Tian JW. Effect of water stress on photosynthesis, chlorophyll fluorescence parameters and water use efficiency of common Reed in the Hexi corridor. *Russ J Plant Physiol*. 2019;66(4):556–63.
- Oxborough K. Using chlorophyll a fluorescence imaging to monitor photosynthetic performance. *Chlorophyll Fluorescence*. 2004;19:409–28.
- Field C, Mooney HA. Leaf age and seasonal effects on light, water, and nitrogen use efficiency in a California shrub. *Oecologia*. 1983;56(2):348–55.
- Huang CP, Yu MY, Sun L, Qin NN, Wei L. Physiological responses of sweet potato seedlings under drought-stress conditions with selenium applications. *J Agricultural Crop Res*. 2020;8:98–112.

32. Wei D, Zhang T, Wang B, Zhang H, Ma M, Li S, Chen THH, Brestic M, Liu Y, Yang X. Glycinebetaine mitigates tomato chilling stress by maintaining high-cyclic electron flow rate of photosystem I and stability of photosystem II. *Plant Cell Rep.* 2022;41(4):1087–101.
33. Schansker G, van Rensen JJS. Performance of active photosystem II centers in photoinhibited pea leaves. *Photosynth Res.* 1999;62(2):175–84.
34. Gomes MTG, da Luz AC, dos Santos MR, do Carmo Pimentel Batitucci M, Silva DM, Falqueto AR. Drought tolerance of passion fruit plants assessed by the OJIP chlorophyll a fluorescence transient. *Scientia Horticulturae* 2012, 142:49–56.
35. Chang X, Zhang S, Cao C, Zhou J, Wang X, Zhang D, Xiang J. Transcriptome analysis and characteristics of drought resistance related genes in four varieties of Foxtail millet [*Setaria italica*]. *Heliyon.* 2024;10(18):e38083.
36. Zhang M, Xu GS, Teng ZY, Liu GJ, Zhang XL. Effects of simulated acid rain on growth and photosynthetic physiological characteristics of *Populus simonii* × *P. nigra*. *J NanJing Forestry Univ.* 2021;45(6):57–64.
37. Zhang HH, Feng P, Yang W, Sui X, Li X, Li W, Zhang RT, Gu SY, Xu N. Effects of flooding stress on the photosynthetic apparatus of leaves of two *Physocarpus* cultivars. *J Forestry Res.* 2018;29(04):1049–59.
38. Henmi T, Miyao M, Yamamoto Y. Release and Reactive-Oxygen-Mediated damage of the Oxygen-Evolving complex subunits of PSII during photoinhibition. *Plant Cell Physiol.* 2004;45(2):243–50.
39. Strasser R, Srivastava A, Govindjee G. Polyphasic chlorophyll a fluorescence transient in plants and cyanobacteria. *Photochem Photobiol.* 2008;61:32–42.
40. Tang G-L, Li X-Y, Lin L-S, Gu Z-Y, Zeng F-J. The chlorophyll a fluorescence characteristic in different types of leaf senescence in *Alhagi sparsifolia*. *J Plant Growth Regul.* 2016;35(4):952–64.
41. Xiong R, Liu S, Considine MJ, Siddique KHM, Lam H-M, Chen Y. Root system architecture, physiological and transcriptional traits of soybean (*Glycine max* L.) in response to water deficit: A review. *Physiol Plant.* 2020;172(2):405–18.
42. Haling RE, Richardson AE, Culvenor RA, Lambers H, Simpson RJ. Root morphology, root-hair development and rhizosheath formation on perennial grass seedlings is influenced by soil acidity. *Plant Soil.* 2010;335(1):47–68.
43. Guo W, Wang G, Gou Q. Effects of sodium salt stress on the growth and biomass allocation of Chenopodiaceae annuals. *Acta Ecol Sin.* 2021;41(16):6633–43.
44. Sathasivan K, Murai HN. Molecular basis of Imidazolinone herbicide resistance in *Arabidopsis thaliana* var Columbia. *Plant Physiol.* 1991;97(3):1044–50.
45. Zhou Q, Liu W, Zhang Y, Liu KK. Action mechanisms of acetolactate synthase-inhibiting herbicides. *Pestic Biochem Physiol.* 2007;89(2):89–96.
46. Délye C. Unravelling the genetic bases of non-target-site-based resistance (NTSR) to herbicides: A major challenge for weed science in the forthcoming decade. *Pest Manag Sci.* 2013;69:176–87.
47. Long N, Orasch T, Zhang S, Gao L, Xu X, Hortschansky P, Ye J, Zhang F, Xu K, Gsaller F. The Zn2Cys6-type transcription factor LeuB cross-links regulation of leucine biosynthesis and iron acquisition in *Aspergillus fumigatus*. *PLoS Genet.* 2018;14(10):e1007762.
48. Niu XH, Liu X, Zhou YF, Xi Z, Su XD. Crystallization of Escherichia coli AHASI regulatory subunit llvN and Co-crystallization llvN with a valine effector. *Progress Biochem Biophys.* 2012;39(1):45–50.
49. Song Q-C, Cao F-Q, Gong Y-Y, Cheng X-Y, Bi X-Y, Liu L-H. Current research progresses of amino acids uptake, transport and their biological roles in higher plants. *J Plant Nutr Fertilizers.* 2012;18(6):1511–21.
50. Dong N-Q, Lin H-X. Contribution of phenylpropanoid metabolism to plant development and plant–environment interactions. *J Integr Plant Biol.* 2021;63(1):180–209.
51. Lam PY, Wang L, Lo C, Zhu FY. Alternative splicing and its roles in plant metabolism. *Int J Mol Sci.* 2022;23(13):7355.
52. Cao D, Zhang W, Yang N, Li Z, Zhang C, Wang D, Ye G, Chen J, Wei X. Proteomic and metabolomic analyses uncover integrative mechanisms in *Sesuvium portulacastrum* tolerance to salt stress. *Front Plant Sci.* 2023;14:1277762.
53. Jia C, Guo B, Wang B, Li X, Yang T, Li N, Wang J, Yu Q. Integrated metabolomic and transcriptomic analysis reveals the role of phenylpropanoid biosynthesis pathway in tomato roots during salt stress. *Front Plant Sci.* 2022;13:1023696.
54. Zhang Q, Li A, Xu B, Wang H, Yu J, Liu J, Jian L, Quan C, Du J. Exogenous melatonin enhances salt tolerance by regulating the phenylpropanoid biosynthesis pathway in common bean at sprout stage. *Plant Stress.* 2024;14:100589.
55. Choi SJ, Lee Z, Kim S, Jeong E, Shim JS. Modulation of lignin biosynthesis for drought tolerance in plants. *Front Plant Sci* 2023, 14.
56. Sedlackova H, Rask M-B, Gupta R, Choudhary C, Somyajit K, Lukas J. Equilibrium between nascent and parental MCM proteins protects replicating genomes. *Nature.* 2020;587(7833):297–302.
57. Miriam SZ, Paulina J, Iwona S. How do plants Cope with DNA damage? A concise review on the DDR pathway in plants. *International J Mol Sci* 2023, 24.

Publisher's note

Springer Nature remains neutral with regard to jurisdictional claims in published maps and institutional affiliations.